

Protective action of nipradilol mediated through S-nitrosylation of Keap1 and H0-1 induction in retinal ganglion cells

著者	Koriyama Yoshiki, Kamiya Marie, Takadera Tsuneo, Arai Kunizo, Sugitani Kayo, Ogai Kazuhiro, Kato Satoru
journal or publication title	Neurochemistry International
volume	61
number	7
page range	1242-1253
year	2012-12-01
URL	http://hdl.handle.net/2297/32831

doi: 10.1016/j.neuint.2012.09.004

Protective action of nipradilol mediated through S-nitrosylation of Keap1 and HO-1 induction in retinal ganglion cells

Yoshiki Koriyama*¹, Marie Kamiya², Tsuneo Takadera³, Kunizo Arai², Kayo Sugitani⁴, Kazuhiro Ogai⁴, Satoru Kato¹

¹Department of Molecular Neurobiology, Graduate School of Medicine, Kanazawa University, 13-1 Takaramachi, Kanazawa 920-8640, Japan

²Department of Clinical Drug Informatics, Faculty of Pharmacy, Institute of Medical, Pharmaceutical and Health Sciences, Kanazawa University, Kanazawa, Japan

³Center of Development for Education, Hokuriku University, Kanazawa, Japan

⁴Division of Health Sciences, Graduate School of Medicine, Kanazawa University, Kanazawa, Japan

Keywords: Nitric oxide, S-nitrosylation, Keap1, retinal ganglion cell, oxidative stress, HO-1

Running title: Protection by Nipradilol via Nrf2/ARE system

Abbreviations:

ARE, antioxidant response element;

ChIP, Chromatin immunoprecipitation;

c-PTIO, 2-(4-carboxyphenyl)-4,4,5,5-tetramethylimidazoline-1-oxyl-3-oxide;

GCLC, glutamate cysteine ligase catalytic subunit;

DeNip, denitro-nipradilol;

4HNE, 4-hydroxy-2-nonenal;
HO-1, heme oxygenase-1;
Keap1, Kelch-like ECH-associated protein;
Nip, nipradilol;
NO, nitric oxide;
NQO-1, NAD(P)H: quinone oxidoreductase-1;
Nrf2, NF-E2-related factor 2;
ONI, optic nerve injury;
RGC, retinal ganglion cell;
SnMP, Sn-mesoporphyrin;

*Address for correspondence: Department of Molecular Neurobiology, Graduate School of Medicine, Kanazawa University, Kanazawa 920-8640, Japan

TEL: 81 76 265 2451

FAX: 81 76 234 4235

E-mail: koriyama@med.kanazawa-u.ac.jp

Abstract

Nipradilol (Nip), which has α 1- and β -adrenoceptor antagonist and nitric oxide (NO)-donating properties, has clinically been used as an anti-glaucomatous agent in Japan. NO mediates cellular signaling pathways that regulate physiological functions. The major signaling mechanisms mediated by NO are cGMP-dependent signaling and protein S-nitrosylation-dependent signalings. Nip has been described as having neuroprotective effects through cGMP-dependent pathway in retinal ganglion cells (RGCs). However, the effect seems to be partial. On the other hand, whether Nip can prevent cell death through S-nitrosylation is not yet clarified. In this study, we therefore focused on the neuroprotective mechanism of Nip through S-nitrosylation. Nip showed a dramatic neuroprotective effect against oxidative stress-induced death of RGC-5 cells. However, denitro-nipradilol, which does not have NO-donating properties, was not protective against oxidative stress. Furthermore, an NO scavenger significantly reversed the protective action of Nip against oxidative stress. In addition, we demonstrated that α 1- or β -adrenoceptor antagonists (prazosin or timolol) did not show any neuroprotective effect against oxidative stress in RGC-5 cells. We also demonstrated that Nip induced the expression of the NO-dependent antioxidant enzyme, heme oxygenase-1 (HO-1). S-nitrosylation of Kelch-like ECH-associated protein by Nip was shown to contribute to the translocation of NF-E2-related factor 2 to the nucleus, and triggered transcriptional activation of HO-1. Furthermore, RGC death and levels of 4-hydroxy-2-nonenal (4HNE) were increased after optic nerve injury *in vivo*. Pretreatment with Nip significantly suppressed RGC death and accumulation of 4HNE after injury through a HO-1 activity-dependent mechanism. These data demonstrate a novel neuroprotective action of Nip against oxidative stress-induced RGC death *in vitro*.

and *in vivo*.

1. Introduction

Nipradilol

(3,4-dihydro-8-(2-hydroxy-3-isopropylamino)-propoxy-3-nitroxy-2H-1-benzopyran; Nip) has vasodilator activity owing to nitric oxide (NO) released from the nitroxy moiety (Adachi et al., 1995). Nip lowers intraocular pressure via its selective α 1-adrenoceptor (Kou et al., 1984; Ohira et al., 1985) and non-selective β -adrenoceptor (Uchida et al., 1983; Kawashima et al., 1984) antagonist properties. Nipradilol is registered as an anti-glaucoma agent in Japan. More recently, a protective effect of Nip has been demonstrated in various neuronal cells (Tomita et al., 2002, Taguchi et al., 2006) including retinal ganglion cells (RGCs; Nakazawa et al., 2002). It has been reported that Nip has a neuroprotective effect on N-methyl-D-aspartate (NMDA)-induced damage to RGCs (Mizuno et al., 2001). The authors concluded that the protective effects of Nip were due to NO-dependent actions because both selective α 1- and non-selective β -adrenoceptor antagonists had no protective effects. However, the mechanism of NO-mediated protection against cell damage is not clear. NO is a gaseous messenger molecule biosynthesized from L-arginine and molecular oxygen by NO synthase. Many reports suggest that excess production of NO plays a crucial role in neuronal cell death (Dawson et al., 1991; Nowicki et al., 1991, Smith et al., 1997), including in death of RGCs (Park et al., 2007). In contrast, several lines of evidence indicate that NO can prevent neuronal death (Chiueh et al., 1999; Lipton, 1999), including death of RGCs (Imai et al., 1997; Mastrodimou et al., 2008), through an NO/cGMP-dependent pathway (Andoh et al., 2002). Tomita and colleagues (2002) reported that the neuroprotective effect of Nip can be partially reversed by inhibiting protein kinase G. We wanted to test whether the neuroprotective action of Nip might

also be mediated by antioxidant effects via the S-nitrosylation pathway, as Naito and collaborators (1994) reported that Nip inhibits H₂O₂-induced lipid peroxidation. Antioxidative proteins, including heme oxygenase-1 (HO-1: EC 1.14.99.3), are induced by activation of Kelch-like ECH-associated protein (Keap1) / NF-E2-related factor 2 (Nrf2) signaling (Kaspar et al., 2009; Kurauchi et al., 2009). Thus, in this study, we specifically investigated the possibility that the neuroprotective mechanism of Nip against oxidative stress and optic nerve injury is mediated through the Keap1/Nrf2 pathway in cultured RGC-5 cells and mouse RGCs, respectively.

2. Material and methods

2.1. Chemicals

Nip and denitro-nipradilol (DeNip) were a kind gift from Kowa (Japan). Timolol maleate, prazosin hydrochloride, and dithiothreitol (DTT) were purchased from Wako (Osaka, Japan). 2-(4-Carboxyphenyl)-4,4,5,5-tetramethylimidazoline-1-oxyl-3-oxide, sodium salt (c-PTIO) and 4', 6-diamino-2-phenylindole (DAPI) were obtained from Dojindo (Kumamoto, Japan). An HO-1 inhibitor, Sn-mesoporphyrin (SnMP), was obtained from Frontier Scientific Inc. (Logan, UT). t-Butyl hydroperoxide (tBOOH) was obtained from Sigma-Aldrich (Tokyo, Japan).

2.2. Cell culture

The cell line RGC-5, a transformed cell line with some ganglion cell characteristics, was originally produced by Dr. N. Agarwal of the University of North Texas Health Science Center and was received from a line maintained by Dr. H. Hara at Gifu Pharmaceutical University (Krishnamoorthy et al., 2001). RGC-5 cells were cultured in

low-glucose Dulbecco's modified Eagle's medium (DMEM) containing 10% fetal bovine serum (FBS), 100 U/ml of penicillin and 100 µg/ml of streptomycin in a humidified atmosphere of 95% air and 5% CO₂ at 37°C. The cells were passaged by trypsinization every 3-4 days. RGC-5 cells (5×10³ cells/ml) were cultured overnight before use. After washing with DMEM, the cells were cultured in medium containing 1% FBS to prevent cell overgrowth.

2.3. Measurement of NO production

The NO indicator, 4-amino-5-methylamino-2',7'-difluorofluorescein diacetate (DAF-FM DA; Daiichi Pure Chemicals, Tokyo, Japan), reacts with NO to form a fluorescent triazole compound. RGC-5 cells were cultured and washed twice with Earle's balanced salt solution (EBSS), treated with Nip or DeNip at 37°C for 1 h, and then 10 µM DAF-FM DA was added to the culture dishes for 30 min to 1 h. The samples were then washed with EBSS and centrifuged at 100 g for 5 min at 23°C. The supernatants were discarded and the pellets resuspended in 500 µl of EBSS. The fluorescence intensity of each cell suspension was measured at an excitation/emission wavelength of 495 nm/515 nm using a Fluoroskan Ascent Fluorescence Reader (Thermo Electron Corporation, Woburn, MA)

2.4. MTT assay

Cell death was estimated using a 3-(4,5-dimethylthiazol-2-yl)-2,5-diphenyltetrazolium bromide (MTT) assay. An aliquot (20 µl) of 2.75 mg/ml MTT in phosphate-buffered saline (PBS) was added to 200 µl of culture medium as described previously (Koriyama et al. 2003). The reaction mixture was incubated at 37°C for 3 h, prior to adding 200 µl

HCl/isopropanol to solubilize the resultant purple formazan product. Absorbance was measured at 550 nm using a Bio-Rad Model 680 Absorbance Microplate Reader (Hercules, CA). Experiments were repeated at least three times and compared with the control experiment.

2.5. RNA isolation and RT-PCR

Total RNA was isolated from RGC-5 cells using Sepasol RNA I (Nacalai Tesque, Japan). Four types of cDNA fragments were obtained by RT-PCR, using an RNA PCR kit (AMV) Ver.3 (TaKaRa, Japan) with the following specific primers: HO-1: 5'-AGCATGCCCCAGGATTTGTC -3'(forward) and 5'-ACCAGCAGCTCAGGGTGAGT -3' (reverse), NAD(P)H: quinine oxidoreductase-1 (NQO-1): 5'- GGCGAGAAGAGCCCTGATTG -3' (forward), 5'-GTGGTGATAGAAAGCAAGGT -3' (reverse), and glutamate cysteine ligase catalytic subunit (GCLC): 5'- TCAAAGGCTTCTCAGCCAGA -3' (forward), 5'-AGATCTCCTTATCGATGGTC-3' (reverse). PCR products were electrophoresed and stained with ethidium bromide. The product bands were quantified using Scion Image software (Scion Corporation, USA), and normalized to the corrected level of glyceraldehyde-3-phosphate dehydrogenase (GAPDH) mRNA.

2.6. S-Nitrosylation analyses

S-Nitrosylation was assessed by a modified biotin switch assay (Jaffrey et al., 2001) using the S-nitrosylated Protein Detection Assay Kit (Cayman Chemical Ann Arbor, Michigan, USA). RGC-5 cells exposed to 20 μ M Nip for 1 h were harvested and lysed at 4°C. Free thiols were blocked by adding S-methyl methanethiosulfonate.

Biotinylation of nitrosothiols was carried out with maleimide-biotin. Biotinylated proteins were further purified by overnight incubation with NeutrAvidin-coupled agarose beads (Pierce-Thermo Scientific). After washing the beads three times with PBS, proteins were recovered by addition of Laemmli sample buffer, and heated at 85°C for 10 min. The amount of S-nitrosylated protein in the samples was determined by western blot analysis using anti-Keap1 (Santa Cruz Biotechnology, CA, USA, 1:500) and anti-caspase-3 (Calbiochem, La Jolla, CA, USA, 1:500) primary antibodies.

2.7. Subcellular fractions of Nrf2 protein

Cells were lysed with hypotonic buffer (10 mM HEPES-KOH (pH7.9), 10 mM KCl, 1.5 mM MgCl₂, 1 mM DTT, 0.5 mM phenylmethylsulfonyl fluoride, protease inhibitor cocktail (Sigma-Aldrich, Tokyo, Japan)) and centrifuged at 10,000 g for 15 min at 4°C. The supernatants comprised the cytoplasmic fraction. The pellets were incubated with a nuclear lysis buffer containing 20 mM HEPES-KOH (pH7.9), 400 mM NaCl, 1.5 mM MgCl₂, 0.2 mM EDTA, 1 mM DTT, 5% glycerol, and protease inhibitor cocktail for 30 min on ice. The lysates were centrifuged at 18,000 g for 15 min at 4°C. The supernatants comprised the nuclear fraction.

2.8. Western blot analysis

RGC-5 cells cultured under various conditions were isolated and aliquots containing 30 µg of protein were subjected to polyacrylamide gel electrophoresis using a 12.5% gel as described previously (Koriyama et al. 2009a). The separated proteins were transferred to a nitrocellulose membrane and incubated sequentially with primary and secondary antibodies. The signal for the Nrf2 protein bands (Cell Signaling Technology, Beverly,

MA) was detected using a BCIP/NBT Kit (KPL, Gaithersburg, MD). An antibody against β -actin (GeneTex, San Antonio, TX, 1:500) was used as an internal standard. The protein bands isolated in samples from cells under various culture conditions were analyzed densitometrically using Scion Image Software (Scion Corp.). All experiments were repeated at least three times.

2.9. Chromatin immunoprecipitation assay

Chromatin immunoprecipitation (ChIP) assays were performed using a ChIP Assay Kit (Upstate/Millipore Corporation, Temecula, CA, USA). Briefly, proteins and DNA were cross-linked with formaldehyde, and cells were lysed in SDS-lysis buffer and then sonicated. To reduce non-specific background, the sheared chromatin was incubated with Protein A agarose/Salmon Sperm DNA. The remaining chromatin was immunoprecipitated with IgG (as control) or Nrf2 antibodies. DNA-protein complexes were eluted from the antibody with elution buffer containing 1% SDS and 0.1 M NaHCO_3 , as well as formaldehyde reversed cross-links by 5 M of NaCl and heating at 65°C for 4 h. DNA was purified and PCR was performed using primers that spanned the HO-1 E1 enhancer (Alam and Cook, 2003). The primers used were: E1, 5'-GATTCCTCACTGCCCTGAA -3' (forward) and 5'- CTTCTGCCCGAGGTAAAGC -3' (reverse). A 1.5% agarose gel with ethidium bromide was used to separate and examine the PCR products.

2.10. Animals and surgery

All experiments on animals were performed in accordance with the guidelines for animal experiments of Kanazawa University. Mice (8-9 weeks old Male, C57BL/6)

were anesthetized by intraperitoneal injection of sodium pentobarbital (30-40 mg/kg body weight). Intravitreal injection of Nip and/or SnMP was performed with a Hamilton microsyringe with 30G needle. The volume of injection was set at 5 μ l of total volume after removal of the same volume of vitreous fluid. The optic nerve was crushed 1 mm away from the eyeball with forceps as described previously (Koriyama et al., 2008). Mice were reared in clear plastic cages and kept under 12 h light–dark cycle at 23°C.

2.11. Immunohistochemistry

Tissue fixation and cryosectioning were performed as described previously (Koriyama et al., 2009b). Briefly, the eyes were enucleated and fixed in 4% paraformaldehyde in 0.1 M phosphate buffer (pH 7.4), and cryoprotected in 5% sucrose for 2 h at 4°C. The sucrose concentration was gradually increased from 5 to 20%. The eyes were then embedded in optimal cutting temperature compound (Tissue Tek; Miles, Eikhart, IN) and cryosectioned at a thickness of 12 μ m. Frozen sections were mounted onto silane-coated glass slides and air-dried. We sampled retinal sections within 300 μ m from the optic disc. After washing and blocking with Blocking One (Nakalai Tesque, Kyoto), retinal sections were incubated with the primary anti-HO-1 antibody (Santa Cruz Biotechnology, 1:300) and anti- β III-tubulin (TUJ1, Abcam, 1:500) at 4°C overnight. The sections were then incubated with Alexa Fluor anti-IgG (Molecular Probes, 1:2,000) at 23°C. As a quantification of HO-1 immunoreactivity, higher-resolution images of two areas at 1500 μ m distance from optic disc were obtained (40 magnifications, 5 mice in a group) as representative data. Assessment of fluorescence intensity of ganglion cell layer was performed using ImageJ software (Wayne Rasband, NIH, Bethesda, MD). In the Nrf2 translocation study, RGC-5 cells were fixed in 0.1%

glutaraldehyde (Wako, Osaka, Japan) for 30 min at 23°C. Nrf2 translocation from cytosol to the nucleus was confirmed by double staining for Nrf2 and DAPI.

2.12. Dot blotting analysis for 4-hydroxy-2-nonenal

To assess the antioxidant effect of Nip, we performed dot blotting analysis for 4-hydroxy-2-nonenal (4HNE), a marker of lipid peroxidation. After 1 day of pretreatment with Nip, in the presence or absence of SnMP, and 4 days of treatment with optic nerve injury, retinal samples were isolated and homogenized. Equal amounts of protein (30 µg) were applied to a Hybri-SLOT apparatus (Gibco BRL) and transferred to a nitrocellulose membrane (Whatman) by vacuum filtration. After blocking with 3% bovine serum albumin for 1 h at 23°C, the samples were incubated with an anti-4HNE antibody (1:100; NOF Corporation) at 4°C overnight, followed by incubation with anti-mouse IgG antibody (Santa Cruz Biotechnology, CA, USA) for 1 h at 23°C. Antibody-bound protein bands were detected using a BCIP/NBT Kit and analyzed densitometrically as described above. All experiments were repeated at least three times.

2.13. Counting of surviving RGCs

RGC survival was evaluated in flat-mounted retinas by immunohistochemistry using a mouse antibody against β III-tubulin (TUJ1, Abcam, 1:500), followed by a fluorescent secondary antibody. Images of 8 prespecified areas of 2 mm away from the optic disc (middle region of the retina) were captured by fluorescent microscopy (under x200 magnification; E600, Nikon) and positive cells were counted using ImageJ software. Cell densities were calculated as mean values of surviving RGCs per 0.14 mm² in 8

specified areas. Data are presented as means \pm S.E.M on five mice per group.

2.14. Terminal transferase-mediated dUTP nick-end labeling (TUNEL) staining

After fixation and cryosection, retinal sections were incubated in 0.1% Triton X-100, as well as 0.1 % sodium citrate for 15 min. Then, sections were further incubated with 20 μ g/ml proteinase K in 10 mM Tris/HCl (pH 7.4) at 37°C for 20 min and rinsed in PBS. DNA fragmentation of cells undergoing apoptosis was detected using an *in situ* cell death detection kit (Roche, Mannheim, Germany), containing terminal transferase and fluorescence dUTP. The retinal sections were incubated in this reaction mixture overnight at 37°C, and rinsed twice in PBS. The number of TUNEL positive cells was counted by fluorescent microscopy (x200 magnification; E600, Nikon) in visual field of middle region of retina (including middle point between optic disc and the edge of retina). Data are presented as means \pm S.E.M on five mice per group (n=25).

2.15. Statistics

All results are reported as means \pm S.E.M for three to five experiments. Differences between groups were analyzed using ANOVA followed by Dunnett's multi-comparison test with PASW Software (SPSS Inc., USA). $P < 0.05$ was considered statistically significant.

3. Results

3.1. Nitric oxide generation by Nip in RGC-5 cells

We first tested whether Nip could induce the generation of NO in RGC-5 cells. Nip (20 μ M) significantly increased the fluorescence intensity of the NO indicator, DAF-FM

DA, in RGC-5 cells at 0.5-1 h after treatment (Figs. 1C and D). DeNip has weak selective α 1-adrenoceptor and non-selective β -adrenoceptor antagonist properties but no NO-donating action (Uchida et al., 1983). Compared with no treatment (Fig. 1A), the same concentration of DeNip did not increase the fluorescence intensity in RGC-5 cells (Fig. 1B)

3.2. Protective effects of Nip against oxidative stress in RGC-5 cells.

To evaluate the neuroprotective effect of Nip against oxidative stress in RGC-5 cells, we constructed oxidative stress model in culture with hydrogen peroxide (H_2O_2), tBOOH, and serum withdrawal. Treatment with 300 μ M H_2O_2 for 24 h induced cell death to 60% of no treated control RGC-5 cells (Fig. 2A). Pretreatment with Nip 4-6 h prior to H_2O_2 exposure produced a maximum protective effect. No protective effect was observed when Nip was applied to RGC-5 cells 0-2 h before H_2O_2 exposure. Additionally, Nip was protective when added to RGC-5 cells following H_2O_2 treatment (Fig. 2B), and this protective effect of Nip was reversed by the NO scavenger, c-PTIO (Fig. 2B). Nip also protected RGC-5 cells from oxidative stress induced by either tBOOH (Fig. 2C) or serum withdrawal (Fig. 2D). Furthermore, c-PTIO significantly suppressed the neuroprotective effect of Nip against both tBOOH (Fig. 2C) and serum withdrawal (Fig. 2D). In contrast, DeNip did not show any neuroprotective effect against serum withdrawal-induced cell death (Fig. 2E).

3.3. HO-1 induction by Nip in RGC-5 cells

Next, we tested whether Nip can induce the expression of the antioxidative enzyme, HO-1, in RGC-5 cells. After 4 h of treatment with 20 μ M Nip, we found that HO-1

mRNA was significantly increased in RGC-5 cells (Fig 3A). Indeed, levels of HO-1 mRNA in RGC-5 cells were shown to be greatest after 4 h treatment with Nip (1.5-fold compared with 0 h; Fig. 3B). Other antioxidative enzymes, such as NQO-1 and GCLC, were not increased for up to 12 h after treatment with Nip (data not shown). HO-1 protein was also increased by 1.7-fold after 4-8 h treatment with Nip, and then declined by 12 h after treatment (Fig. 3C). This peak in HO-1 expression at 4-8 h following treatment with Nip is consistent with the maximum protective effect of Nip when applied 4-6 h before H₂O₂ exposure (Fig. 2A). In the presence of the HO-1 specific inhibitor, SnMP (10 μM), the neuroprotective effect of Nip against H₂O₂ decreased from 80% to 60% (Fig.3D). SnMP alone did not affect the viability of RGC-5 cells, either in the presence or absence of H₂O₂. The neuroprotective effect of Nip against serum deprivation was also reduced by SnMP in RGC-5 cells (data not shown).

3.4. α1- and β-adrenoceptor antagonists are not protective against oxidative stress in RGC-5 cells.

We examined the possible involvement of α1-adrenoceptors and β-adrenoceptors in the Nip-induced neuroprotection of RGC-5 cells using the specific antagonists, prazosin and timolol, respectively. Results from RT-PCR confirmed that RGC-5 cells express both α1- and β-adrenoceptors (data not shown). Neither prazosin (Fig. 4A) nor timolol (Fig. 4B) prevented H₂O₂-induced death of RGC-5 cells. Furthermore, prazosin and timolol did not show any protective effect against serum withdrawal-induced cell death (data not shown). DeNip, prazosin or timolol did not alter HO-1 mRNA expression for 12 h (Fig. 4C). These results suggest that the neuroprotective effect of Nip is not mediated by blocking of α1- and β-adrenoceptors.

3.5. Nip induces NO/S-nitrosylation dependent translocation of Nrf2 to the nucleus in RGC-5 cells.

To test the involvement of the Keap1/Nrf2 system in the Nip-induced increase in HO-1, we analyzed the levels of Nrf2 in the nucleus of RGC-5 cells under three conditions: (i) no treatment (Figs. 5A-C), (ii) treatment with 20 μ M Nip (Figs. 5D-F), and (iii) treatment with 20 μ M Nip plus 100 μ M c-PTIO (Figs. 5G-I). Following treatment, cells were stained for Nrf2 (Figs. 5A, D and G) and with DAPI (Fig. 5B, E and H), and images of this staining were merged (Fig. 5C, F and I) to visualize Nrf2 in nuclei. In non-treated RGC-5 cells, Nrf2 in the cytoplasm was diffusely stained in the cytoplasm (Fig. 5A). Nip induced translocation of Nrf2 into the nucleus (Fig. 5D). This Nip-induced increase of Nrf2 staining in nuclei was dramatically blocked by c-PTIO treatment (Fig. 5G). Nuclear fraction analysis quantitatively confirmed this translocation of Nrf2 from the cytoplasm to the nucleus. The nuclear level of Nrf2 protein was increased at 2 h following Nip treatment. DTT, an S-nitrosylation blocker, significantly inhibited nuclear translocation of Nrf2 (Fig. 5J). DTT and c-PTIO alone did not affect Nrf2 translocation as compared with no treatment. The proportion of Nrf2 that translocated to the nuclei was calculated and graphed in Fig. 5K. These results suggest that Nip-mediated translocation of Nrf2 to the nucleus is dependent on NO/S-nitrosylation pathways.

3.6. Nip stimulated Keap1 S-nitrosylation and Nrf2 binding to the E1 enhancer in RGC-5 cells

To further confirm the association between HO-1 expression and the NO/S-nitrosylation

pathway, we investigated the effects of an NO scavenger and S-nitrosylation blocker on HO-1 induction by Nip. Nip (20 μ M) increased HO-1 mRNA 1.6-fold within 4 h following treatment (Fig. 6A and B). This increase of HO-1 mRNA was blocked by c-PTIO (Fig. 6A) and DTT (Fig. 6B). Next, we investigated whether Nip modified the oxidative state of the intracellular sensor molecule, Keap1. After removal of free thiols, S-nitrosylation of Keap1 was detected by biotinylating nitrosothiols and isolated with avidin-coupled beads, and was then measured by western blotting with an anti-Keap1 antibody. Nip treatment increased S-nitrosylated Keap1 1.8-fold compared with no treatment (Fig. 6C). The increase of S-nitrosylation of Keap1 by Nip was significantly suppressed by pretreatment with either c-PTIO or DTT. This effect was specific to Keap1 but not to caspase-3 (Fig. 6D). To further assess the involvement of Nrf2 on HO-1 gene expression, we determined binding of Nrf2 to the HO-1 enhancer E1 element of genomic HO-1 DNA. ChIP assays with an antibody directed against Nrf2 showed high binding of Nrf2 to the E1 enhancer motif. Nip treatment for 2 h significantly enhanced Nrf2 binding to the E1 enhancer by about 3-fold (Fig. 6E). Pretreatment with c-PTIO for 1 h completely reversed the binding of Nrf2 to the E1 enhancer. The ChIP assay performed with IgG did not show increased binding of Nrf2 to the E1 enhancer, compared with no treatment (Fig. 6E).

3.7. Nip prevents 4HNE accumulation in mouse RGCs after optic nerve injury.

To further validate the protective effect of Nip in mouse RGCs *in vivo* after optic nerve injury, we investigated the effect of intraocular injection of Nip on HO-1 expression. Figures 7 (A) to (I) show HO-1 immunohistochemistry in the mouse retina. Panels (A-C) show the untreated retina. Panels (D-F) show retina treated with Nip at 1 day.

Strong HO-1 immunoreactivity was observed in the mouse RGC layer after treatment with 0.3 nmol Nip (Fig. 7D), compared with no treatment (Fig. 7A). The Nip-induced increase of HO-1 expression in the ganglion cell layer was shown to localize in RGCs by staining with TUJ-1 (Fig. 7E). The colocalization of HO-1 and TUJ-1 in the RGCs can be seen in the merged images (Fig. 7F). Levels of HO-1 protein decreased to control levels within 3 days after Nip treatment (Fig. 7G-I). Quantification of HO-1 expression is shown in Fig. 7J. We also measured the accumulation of 4HNE, a final product of lipid peroxidation (Koriyama et al., 2009b), following optic nerve injury in the mouse. Optic nerve injury increased 4HNE accumulation in the mouse retina by 2.5-fold at 7 days post-injury, compared with the intact retina (Fig. 7K). Nip significantly decreased the levels of 4HNE. The Nip-mediated decrease in 4HNE accumulation after nerve injury was significantly suppressed by co-injection of 0.15 nmol SnMP (Fig. 7K). Intraocular treatment with Nip or SnMP alone did not alter 4HNE levels compared with no treatment.

3.8. Nip prevents RGC death after optic nerve injury.

Staining with TUJ1 revealed that optic nerve injury induced apoptotic cell death of RGCs 10 days after injury (Figs. 8B and E, and Table 1) compared with the intact retina (Fig. 8A). The death of RGCs after injury was clearly blocked by pretreatment with 0.3 nmol Nip (Figs. 8C and E). This neuroprotective effect of Nip in mouse RGCs following nerve injury was not seen with treatment with 0.3 nmol Nip plus 0.15 nmol SnMP (Figs. 8D and E). SnMP alone did not affect RGC death compared with no treatment. Figures 9(A) to (D) show TUNEL staining in the mouse retina. Optic nerve crush induced apoptotic cell death of RGCs with TUNEL staining 10 days after injury

(Fig. 9B) compared with the intact retina (Fig. 9A). The cell death of RGCs after injury was clearly blocked by pre-treatment with Nip (Fig. 9C). This neuroprotective effect of Nip in RGCs following nerve crush could not be seen by Nip plus SnMP (Fig. 9D). SnMP alone did not affect RGC cell death (data not shown). Figure 9(E) illustrates the quantitative data of RGCs cell death after ONI.

4. Discussion

4.1. The antioxidative effect of Nip is mediated through NO generation and increased HO-1 expression.

In the present study, we demonstrated that the potent NO donor, Nip, is neuroprotective against oxidative stress models in the RGC-5 cell line and mouse RGCs *in vivo*. Since DeNip, which does not release NO, did not induce HO-1 expression or protect RGC-5 cells against oxidative stress, we suggest that the neuroprotective effect of Nip is mediated through the generation of NO.

Nip provides neuroprotection against axotomy of rat RGCs (Mizuno et al., 2001; Nakazawa et al., 2002) and prevents apoptosis mediated by NMDA receptor excitotoxicity in the retina, mainly through the production of NO gas (Kitaoka et al., 2002). The neuroprotective role of Nip may also be mediated through antiapoptotic pathways, specifically through down-regulation of Bax and caspase-9 (Ando et al., 2005). Because Nip has selective α 1- and non-selective β -adrenoceptor antagonist properties, we used prazosin as an α 1-blocker and timolol as a β -blocker. However, neither prazosin nor timolol induced HO-1 or influenced the survival rate in our oxidative stress models, despite RGC-5 cells having both α 1- and β -adrenoceptors (data not shown). Nip has previously been shown to have a neuroprotective effect against

NMDA treatment of RGCs (Mizuno et al., 2001) and axotomy (Nakazawa et al., 2002), which was not reversed by prazosin or timolol. Moreover, DeNip did not induce expression of antioxidative enzymes or show any neuroprotective effect against oxidative stress in the present study. These results indicate that the protective effect of Nip works in a NO-dependent fashion.

4.2. Nip induces Keap1 S-nitrosylation and HO-1 protein expression through Nrf2 translocation to the nucleus in RGC-5 cells.

In general, NO mediates neuroprotection through two main signaling pathways: the NO/cGMP pathway (Andoh et al., 2002) and the S-nitrosylation pathway (Sun et al., 2006). Although the neuroprotective effect of Nip was previously reported to be mediated through a cGMP-dependent protein kinase pathway (Tomita et al., 2002), the effect seems to be partial. In addition, Naito and colleagues (1994) reported that Nip inhibited hydrogen peroxide-induced lipid peroxidation. Because of these previous findings, we focused on the S-nitrosylation-dependent antioxidative mechanism of Nip. NO-donating aspirin induces antioxidative enzymes and shows antioxidant effects in cancer cells (Gao et al., 2006). Buckley and others (2003, 2008) reported that NO stimulates Nrf2 nuclear translocation in vascular endothelium. NO also activates Keap1/Nrf2 by S-nitrosylation in carcinoma cells (Li et al., 2009). However, whether Nip induces S-nitrosylation of Keap1 and antioxidative enzymes is unclear. Thus, we investigated the signaling pathway leading to induction of antioxidative enzymes by Nip. We showed that Nip induced HO-1. HO-1 (Maines 1988; Poss and Tonegawa 1997) is an enzyme that degrades intracellular heme to free iron, carbon monoxide, and biliverdin. Carbon monoxide plays a significant role in anti-apoptosis and

anti-inflammation (Otterbein et al., 2000, 2003). Furthermore, bilirubin, converted from biliverdin (Nishimura et al., 1996), acts as a strong reactive oxygen species scavenger and attenuates lipid peroxidation related to 4HNE (Deguchi et al., 2008). Biliverdin also exerts anti-inflammatory and neuroprotective effects (Hung et al., 2010). In this study, SnMP partially reversed the Nip-mediated protection against oxidative stress.

Furthermore, an *in vivo* study showed that Nip can dramatically suppress injury-induced 4HNE accumulation and that SnMP can significantly reverse this effect. HO-1 is primarily involved in this survival effect against oxidative stress. Taken together, these data strongly suggest that the neuroprotective action of Nip against oxidative stress is caused by NO generation following antioxidant HO-1 induction in RGC-5 cells.

Next, we studied the possibility that the induction of HO-1 by Nip is mediated through the Keap1/Nrf2 pathway. It is known that Nrf2 is a key transcription factor for the induction of antioxidative enzymes (Kaspar et al., 2009). Nip rapidly induced translocation of Nrf2 to the nucleus within 2 h of treatment. Translocation of Nrf2 was dependent on NO/S-nitrosylation, because c-PTIO and DTT significantly blocked the translocation of Nrf2, as well as the Nip-mediated neuroprotection and increase in HO-1 expression. The induction of HO-1 is known to be dependent on the presence of antioxidant response element sites containing an E1 enhancer region in the HO-1 promoter (Alam and Cook, 2003). Using the ChIP method, we confirmed increased levels of Nrf2 bound to the E1 enhancer of the HO-1 promoter in RGC-5 cells treated with Nip. The translocation of Nrf2 from the cytoplasm to the nucleus is regulated by the intracellular sensor protein, Keap1 (Li et al., 2009, Buckley et al., 2008). In this study, we demonstrated that Nip certainly increased S-nitrosylation of Keap1 by 1.7-fold compared with no treatment. Tomita and collaborators (2002) discussed the

possibility that the neuroprotective action of Nip against serum deprivation in PC12 cells might be caused by caspase-3 S-nitrosylation. However, this was not the case in RGC-5 cells. The results presented here demonstrate for the first time that the neuroprotective action of Nip is caused by induction of the HO-1 antioxidant protein in RGC-5 cells through activation of the Keap1/Nrf2 pathway by Keap1 S-nitrosylation.

4.3. Neuroprotective action of Nip in mouse RGCs after nerve injury in vivo

In our previous paper (Homma et al., 2007), we reported that more than half of adult rat RGCs became apoptotic 7 days after nerve injury. The death of RGCs following nerve crush was partly caused by hydroxyl radicals or super oxide anions (Levkovitch-verbin et al., 2000). Therefore, cell death was blocked by antioxidants such as N-acetylcysteine (Castagne and Clarke 1996). In this study, optic nerve injury increased 4HNE accumulation in the retina. Therefore, we studied mouse RGCs after nerve injury as an *in vivo* model of oxidative stress. Intraocular injection of Nip specifically induced HO-1 expression in the RGCs 1 day post-injection. These results suggest that Nip induced HO-1 expression via NO generation. Further studies are needed to evaluate the molecular signaling involved in this Nip-mediated HO-1 induction in the retina *in vivo*. RGC death after nerve injury was significantly reduced by Nip. This protection depended on HO-1 induction, because the protective action of Nip was attenuated by co-injection with a HO-1 inhibitor. The Nip-induced decrease in 4HNE accumulation was also significantly suppressed by the HO-1 inhibitor. These results demonstrate for the first time that Nip protects mouse RGC death against oxidative stress *in vitro* and *in vivo* through the induction of the antioxidant HO-1 via the Keap1/Nrf2 pathway. This novel neuroprotective action of Nip may shed an additional light as its

anti-glaucomatous agents.

Acknowledgement

We thank to Ms Sachiko Higashi and Ms Tomoko Kano for administrative and technical assistance. This work was supported by Grants-in-Aid for Scientific Research to Y.K. (No. 22791651), S.K. (No. 22300109 and No. 23650163) and K.S. (No.23618006) from the Ministry of Education, Culture, Sports, Science, and Technology, Japan and Adaptable and Seamless Technology transfer Program through target-driven R&D of the Japan Science and Technology Agency (to Y.K.).

References

- Adachi, T., Hori, S., Miyazaki, K., Takahashi, E., Nakagawa, M., Udagawa, A., Hayashi, N., Aikawa N., Ogawa, S., 1995. Rapid increase in plasma nitrite concentration following intravenous administration of Nipradilol. *Eur. J. Pharmacol.* 286, 201-204.
- Alam, J., Cook, J. L., 2003. Transcriptional regulation of the heme oxygenase-1 gene via the stress response element pathway. *Curr. Pharm. Des.* 9, 2499-2511.
- Ando, A., Yamazaki, Y., Kaneko, S., Miyake, M., Nambu, R., Taomoto, M., Unezaki, S., Okuda-Ashitaka, E., Okumura, T., Ito, S., Matsumura, M., 2005. Cytoprotection by Nipradilol, an anti-glaucomatous agent, via down-regulation of apoptosis related gene expression and activation of NF-kappaB. *Exp. Eye. Res.* 80, 501-507.
- Andoh, T., Chock, P.B., Chiueh, C.C., 2002. Preconditioning-mediated neuroprotection: role of nitric oxide, cGMP, and new protein expression. *Ann. NY Acad. Sci.* 962, 1-7.

- Buckley, B. J., Marshall, Z. M., Whorton A. R., 2003. Nitric oxide stimulates Nrf2 nuclear translocation in vascular endothelium. *Biochem. Biophys. Res. Commun.* 307, 973-979.
- Buckley, B. J., Li, S., Whorton, A. R., 2008. Keap1 modification and nuclear accumulation in response to S-nitrosocysteine. *Free Radic. Biol. Med.* 44, 692-698.
- Castagné, V., Clarke P. G., 1996. Axotomy-induced retinal ganglion cell death in development: its time-course and its diminution by antioxidants. *Proc. Biol. Sci.* 263, 1193-1197.
- Chiueh, C. C., 1999. Neuroprotective properties of nitric oxide. *Ann. N. Y. Acad. Sci.* 890, 301-311.
- Dawson, V. L., Dawson, T. M., London, E. D., Brecht, D. S., Snyder, S. H., 1991. Nitric oxide mediates glutamate neurotoxicity in primary cortical cultures. *Proc. Natl. Acad. Sci. USA.* 88, 6368-6371.
- Deguchi, K., Hayashi, T., Nagotani, S., Sehara, Y., Zhang, H., Tsuchiya, A., Ohta, Y., Tomiyama, K., Morimoto, N., Miyazaki, M., Huh, N.H., Nakao, A., Kamiya, T., Abe, K., 2008. Reduction of cerebral infarction in rats by biliverdin associated with amelioration of oxidative stress. *Brain Res.* 1188, 1-8.
- Gao, J., Kashfi, K., Liu, X., Rigas, B., 2006. NO-donating aspirin induces phase II enzymes *in vitro* and *in vivo*. *Carcinogenesis* 27, 803-810.
- Homma, K., Koriyama, Y., Mawatari, K., Higuchi, Y., Kosaka, J., Kato, S., 2007. Early downregulation of IGF-I decides the fate of rat retinal ganglion cells after optic nerve injury. *Neurochem. Int.* 50, 741-748.
- Hung, S., Y., Liou, H. C., Fu, W. M., 2010. The mechanism of heme oxygenase-1 action involved in the enhancement of neurotrophic factor expression. *Neuropharmacology*

58, 321-329.

Imai, N., Tsuyama, Y., Murayama, K., Adachi-Usami, E., 1997. Protective effect of nitric oxide on ischemic retina. *Nihon Ganka Gakkai Zasshi* 101, 639-643.

Jaffrey, S. R., Erdjument-Bromage, H., Ferris, C. D., Tempst, P., Snyder, S. H., 2001. Protein S-nitrosylation: a physiological signal for neuronal nitric oxide. *Nat. Cell Biol.* 3, 193-197.

Kaspar, J. W., Niture, S. K., Jaiswal, A. K., 2009. Nrf2:INrf2 Keap1 signaling in oxidative stress. *Free Radic. Biol. Med.* 47, 1304-1309.

Kawashima, K., Watanabe, T. X., Sokabe H., 1984. Pharmacodynamic and pharmacokinetic studies on prizidilol and Nipradilol K-351, antihypertensive drugs with combined vasodilator and beta-adrenoceptor blocking actions, in rabbits. *Jpn. J. Pharmacol.* 36, 519-526.

Kitaoka, Y., Kumai, T., Isenoumi, K., Kobayashi, S., Ueno, S., 2002. Nipradilol induces vasodilation of canine isolated posterior ciliary artery via stimulation of the guanylyl cyclase-cGMP pathway. *Life Sci.* 71, 1115-1124.

Koriyama, Y., Chiba, K., Mohri, T., 2003. Propentofylline protects beta-amyloid protein-induced apoptosis in cultured rat hippocampal neurons. *Eur. J. Pharmacol.* 458, 235-241.

Koriyama, Y., Tanii, H., Ohno, M., Kimura, T., Kato, S., 2008. A novel neuroprotective role of a small peptide from flesh fly, 5-S-GAD in the rat retina *in vivo*. *Brain Res.* 1240, 196-203.

Koriyama, Y., Yasuda, R., Homma, K., Mawatari, K., Nagashima, M., Sugitani, K., Matsukawa, T., Kato, S., 2009a. Nitric oxide-cGMP signaling regulates axonal elongation during optic nerve regeneration in the goldfish *in vitro* and *in vivo*. *J.*

- Neurochem. 110, 890-901.
- Koriyama, Y., Ohno, M., Kimura, T., Kato, S., 2009b. Neuroprotective effects of 5-S-GAD against oxidative stress-induced apoptosis in RGC-5 cells. *Brain Res.* 1296, 187-195.
- Kou, K., Ibengwe, J., Suzuki, H., 1984. Effects of alpha-adrenoceptor antagonists on electrical and mechanical responses of the isolated dog mesenteric vein to perivascular nerve stimulation and exogenous noradrenaline. *Naunyn Schmiedeberg's Arch. Pharmacol.* 326, 7-13.
- Krishnamoorthy, R.R., Agarwal, P., Prasanna, G., Vopat, K., Lambert, W., Sheedlo, H.J., Pang, I.H., Shade, D., Wordinger, R.J., Yorio, T., Clark, A.F., Agarwal, N., 2001. Characterization of a transformed rat retinal ganglion cell line. *Brain Res. Mol. Brain Res.* 86, 1-12.
- Kurauchi, Y., Hisatsune, A., Isohama, Y., Katsuki, H., 2009. Nitric oxide-cyclic GMP signaling pathway limits inflammatory degeneration of midbrain dopaminergic neurons: cell type-specific regulation of heme oxygenase-1 expression. *Neuroscience* 158, 856-866.
- Levkovitch-Verbin, H., Harris-Cerruti, C., Groner, Y., Wheeler, L. A., Schwartz, M., Yoles, E., 2000. RGC death in mice after optic nerve crush injury: oxidative stress and neuroprotection. *Invest. Ophthalmol. Vis. Sci.* 41, 4169-4174.
- Li, C. Q., Kim, M. Y., Godoy, L. C., Thiantanawat, A., Trudel, L. J., Wogan, G. N., 2009. Nitric oxide activation of Keap1/Nrf2 signaling in human colon carcinoma cells. *Proc. Natl. Acad. Sci. USA.* 106, 14547-14551.
- Lipton, S. A., 1999. Neuronal protection and destruction by NO. *Cell. Death. Differ.* 6, 943-951.

- Maines, M.D., 1988. Heme oxygenase: function, multiplicity, regulatory mechanisms, and clinical applications. *FASEB. J.* 2, 2557-2568.
- Mastrodimou, N., Kiagiadaki, F., Thermos, K., 2008. The role of nitric oxide and cGMP in somatostatin's protection against retinal ischemia. *Invest. Ophthalmol. Vis. Sci.* 49, 342-349.
- Mizuno, K., Koide, T., Yoshimura, M., Araie, M., 2001. Neuroprotective effect and intraocular penetration of Nipradilol, a beta-blocker with nitric oxide donative action. *Invest. Ophthalmol. Vis. Sci.* 42, 688-694.
- Naito, A., Aniya, Y., Sakanashi, M., 1994. Antioxidative action of the nitrovasodilator nicorandil: inhibition of oxidative activation of liver microsomal glutathione S-transferase and lipid peroxidation. *Jpn. J. Pharmacol.* 65, 209-213.
- Nakazawa, T., Tomita, H., Yamaguchi, K., Sato, Y., Shimura, M., Kuwahara, S., Tamai, M., 2002. Neuroprotective effect of Nipradilol on axotomized rat retinal ganglion cells. *Curr. Eye Res.* 24, 114-122.
- Nishimura, R. N., Dwyer, B. E., Lu, S. Y., 1996. Localization of heme oxygenase in rat retina: effect of light adaptation. *Neurosci. Lett.* 205, 13-16.
- Nowicki, J. P., Duval, D., Poignet, H., Scatton B., 1991. Nitric oxide mediates neuronal death after focal cerebral ischemia in the mouse. *Eur. J. Pharmacol.* 204, 339-340.
- Ohira, A., Wada, Y., Fujii, M., Nakamura, M., Kasuya, Y., Hamada, Y., Shigenobu, K., 1985. Effects of Nipradilol K-351 on alpha-adrenoceptor mediated responses in various isolated tissues. *Arch. Int. Pharmacodyn. Ther.* 278, 61-71.
- Otterbein, L. E., Bach, F. H., Alam, J., Soares, M., Tao, L.H., Wysk, M., Davis, R. J., Flavell, R. A., Choi, A. M., 2000. Carbon monoxide has anti-inflammatory effects involving the mitogen-activated protein kinase pathway. *Nat. Med.* 6, 422-428.

- Otterbein, L.E., Zuckerbraun, B.S., Haga, M., Liu, F., Song, R., Usheva, A., Stachulak, C., Bodyak, N., Smith, R.N., Csizmadia, E., Tyagi, S., Akamatsu, Y., Flavell, R.J., Billiar, T.R., Tzeng, E., Bach, F.H., Choi, A.M., Soares, M.P., 2003. Carbon monoxide suppresses arteriosclerotic lesions associated with chronic graft rejection and with balloon injury. *Nat. Med.* 9, 183-190.
- Park, S. H., Kim, J. H., Kim, Y. H., Park, C. K., 2007. Expression of neuronal nitric oxide synthase in the retina of a rat model of chronic glaucoma. *Vision Res.* 47, 2732-2740.
- Poss, K.,D., Tonegawa, S., 1997. Reduced stress defense in heme oxygenase 1-deficient cells. *Proc. Natl. Acad. Sci. USA.* 94, 10925-10930.
- Smith, M. A., Richey Harris, P. L., Sayre, L. M., Beckman, J. S., Perry, G., 1997. Widespread peroxynitrite-mediated damage in Alzheimer's disease. *J. Neurosci.* 17, 2653-2657.
- Sun, J., Steenbergen, C., Murphy, E., 2006. S-nitrosylation: NO-related redox signaling to protect against oxidative stress. *Antioxid. Redox Signal.* 8,1693-1705.
- Taguchi, R., Shirakawa, H., Yamaguchi, T., Kume, T., Katsuki, H., Akaike, A., 2006. Nitric oxide-mediated effect of nipradilol, an α - and β -adrenergic blocker, on glutamate neurotoxicity in rat cortical cultures. *Eur. J. Pharm.* 535, 86-94.
- Tomita, H., Nakazawa, T., Sugano, E., Abe, T., Tamai, M., 2002. Nipradilol inhibits apoptosis by preventing the activation of caspase-3 via S-nitrosylation and the cGMP-dependent pathway. *Eur. J. Pharmacol.* 452, 263-268.
- Uchida, Y., Nakamura, M., Shimizu, S., Shirasawa, Y., Fujii, M., 1983. Vasoactive and beta-adrenoceptor blocking properties of 3,4-dihydro-8-2-hydroxy-3-isopropylamino propoxy-3-nitroxy-2H-1-benzopyran K-351, a new antihypertensive agent. *Arch. Int.*

Pharmacodyn. Ther. 262, 132-149.

Figure legends

Fig 1. Nitric oxide (NO) production by Nip in RGC-5 cells.

NO production by Nip was evaluated in RGC-5 cells by DAF-FM DA staining (A-C).

(A) Non-treated cells. (B) Cells treated with 20 μM DeNip for 1h. (C) Cells treated with 20 μM Nip for 1h. Scale bar = 10 μm . (D) Quantitative data of fluorescence intensity were measured by a fluorescence plate reader. $*P < 0.01$ vs 0 h (n=6). X: no treatment, closed circle: DeNip, open circle: Nip.

Fig 2. Protective effect of Nip against oxidative stress-induced death of RGC-5 cells.

(A) Pretreatment with Nip for various time periods prior to 300 μM H_2O_2 exposure. A 4-6 h pretreatment with Nip (20 μM) was sufficient to prevent H_2O_2 -induced cell death.

$*P < 0.01$ vs no treatment (n=6). (B) NO-dependent neuroprotective effect of Nip

against H_2O_2 -induced neurotoxicity in RGC-5 cells. $*P < 0.01$ vs no treatment, $+P <$

0.01 vs H_2O_2 alone. (C) NO-dependent neuroprotective effect of Nip against

tBOOH-induced neurotoxicity in RGC-5 cells. $*P < 0.01$ vs no treatment, $+P < 0.01$ vs

tBOOH treatment (n=6). (D) NO-dependent neuroprotective effect of Nip against serum

deprivation-induced neurotoxicity in RGC-5 cells. $*P < 0.01$ vs no treatment, $+P < 0.01$

vs serum deprivation (n=6). (E) DeNip did not show a neuroprotective effect against

serum deprivation-induced neurotoxicity in RGC-5 cells. $*P < 0.01$ vs no treatment

(n=6).

Fig 3. Nip induces HO-1 and HO-1 activity is necessary for the protective effect of Nip against oxidative stress in RGC-5 cells.

(A) Nip induced HO-1 mRNA expression in a dose-dependent manner after 4 h

treatment. $*P < 0.01$ vs 0 μM (n=3). (B) Upregulation of HO-1 mRNA in RGC-5 cells after Nip treatment. $*P < 0.01$ vs 0 h (n=3). (C) Upregulation of HO-1 protein in RGC-5 cells after Nip treatment. $*P < 0.01$ vs 0 h (n=3). (D) A HO-1 inhibitor, Sn-mesoporphyrin (SnMP), canceled the neuroprotection afforded by Nip against H_2O_2 . $*P < 0.05$, $**P < 0.01$ vs no treatment, $+P < 0.01$ vs H_2O_2 treatment, $\#P < 0.01$ vs H_2O_2 plus Nip treatment (n=6).

Fig 4. α 1- and β -adrenoceptor antagonists did not show a protective effect against oxidative stress-induced RGC-5 cell death. (A) The α 1-adrenoceptor antagonist, prazosin, did not affect H_2O_2 -induced RGC-5 cell death. $*P < 0.01$ vs no treatment (n=6). (B) The β -adrenoceptor antagonist, timolol, did not affect H_2O_2 -induced RGC-5 cell death. $*P < 0.01$ vs no treatment (n=6). (C) DeNip, prazosin, and timolol did not induce HO-1 mRNA expression.

Fig 5. NO/S-nitrosylation dependent translocation of Nrf2 to the nucleus by Nip in RGC-5 cells.

(A, D, G) Immunohistochemical staining for Nrf2. Treatment with c-PTIO at 1 h prior to addition of Nip. (A) No treatment. Scale bar = 10 μm . (D) Treatment with 20 μM Nip for 2 h. (G) Treatment with Nip plus c-PTIO. (B, E, H) DAPI staining. (C, F, I) Merged images. (J) Levels of Nrf2 protein in nuclear fractions treated with Nip. $*P < 0.01$ vs no treatment, $+P < 0.01$ vs Nip treatment (n=3). (K) The proportion of Nrf2 translocation to the nuclei was calculated and graphed. $*P < 0.01$ vs no treatment, $+P < 0.01$ vs Nip (n=25).

Fig 6. Nip induces S-nitrosylation of Keap1 but not caspase-3 in RGC-5 cells. (A) c-PTIO canceled the Nip-mediated increase in HO-1 mRNA. $*P < 0.01$ vs no treatment (n=3). (B) DTT attenuated the HO-1 mRNA induction by Nip. $*P < 0.01$ vs no treatment (n=3). (C) S-nitrosylation of Keap1 by Nip. RGC-5 cells were exposed to 20 μ M Nip for 1 h before undergoing the biotin-switch assay of protein. $*P < 0.01$ vs no treatment, $+P < 0.01$ vs Nip treatment (n=3). (D) Nip did not induce S-nitrosylation of caspase-3 in RGC-5 cells (n=3). (E) ChIP assay demonstrates binding of Nrf2 to the HO-1 E1 enhancer following treatment with Nip for 2 h, with or without c-PTIO pretreatment for 1 h. The band shows PCR products of the E1 enhancer.

Fig 7. HO-1 induction and prevention of nerve injury-induced 4HNE accumulation by Nip in mouse retina. (A-I) Nip induction of HO-1 in the mouse retina. (A, D, G) Immunohistochemistry for HO-1 at 0 days (A), 1 day (D) and 3 days (G). (B, E, H) TUJ-1-positive RGCs at 0 days (B), 1 day (E) and 3 days (H). (C, F, I) Merged images at 0 days (C), 1 day (F) and 3 days (I). Scale bar = 20 μ m. INL; inner nuclear layer, GCL; ganglion cell layer. (J) The level of HO-1 protein expression was quantified by analysis of fluorescence intensity and represented on the graph. $*P < 0.01$ vs 0 days (n=10). (K) Nip-mediated prevention of nerve injury-induced 4HNE accumulation via HO-1 activation. 4HNE production was measured by dot blotting analyses with an anti-4HNE antibody. $*P < 0.01$ vs intact retina, $+P < 0.01$ vs injury, $\#P < 0.01$ injury plus Nip treatment (n=3). ONI; optic nerve injury.

Fig 8. Nip-mediated RGC survival after optic nerve injury is dependent on HO-1. (A-D) Retinal whole mounts immunostained with TUJ-1 to visualize surviving RGCs

densities. (A) Intact retina. Scale bar= 20 μm . (B) Injury. (C) ONI plus Nip treatment. (D) ONI plus Nip plus SnMP treatment. (E) Quantification of surviving RGCs (Number of RGCs/ mm^2). * $P < 0.01$ vs intact retina, + $P < 0.01$ vs injury, # $P < 0.01$ vs injury plus Nip treatment ($n = 8$). ONI; optic nerve injury.

Fig. 9 Neuroprotective effect of Nip in the rat retina *in vivo*. (A–D) TUNEL staining in retina after optic nerve injury for 10 days. (A) Intact retina, (B) optic nerve injured retina, (C) ONI plus Nip, (D) ONI plus Nip with SnMP. Scale bar = 100 μm . INL; inner nuclear layer, GCL; ganglion cell layer, Arrows indicate TUNEL-positive cells. (E) Graphical representation of the number of TUNEL-positive cells in the GCL per visual fields (x200 magnification). * $P < 0.01$ vs intact retina, + $P < 0.01$ vs injury, # $P < 0.01$ vs injury plus Nip ($n = 25$). ONI; optic nerve injury.

Fig.1

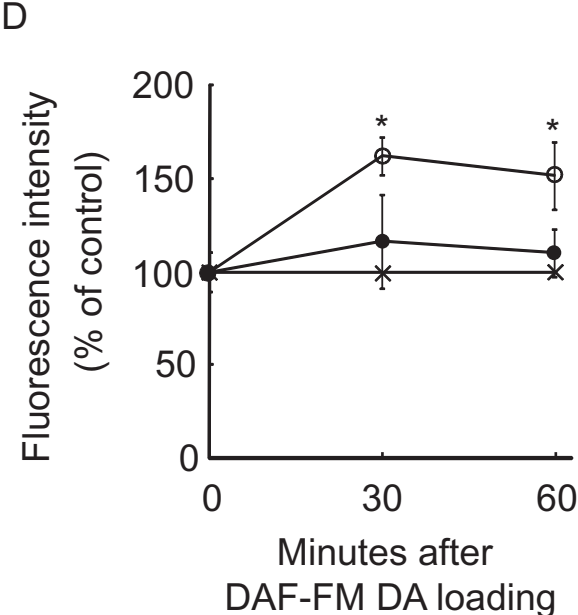
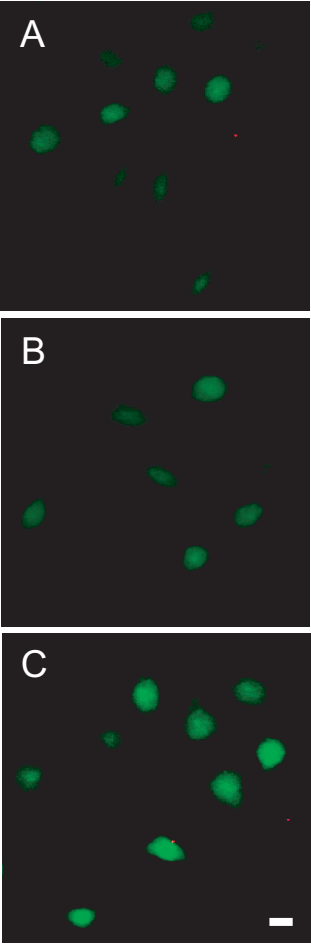


Fig. 2

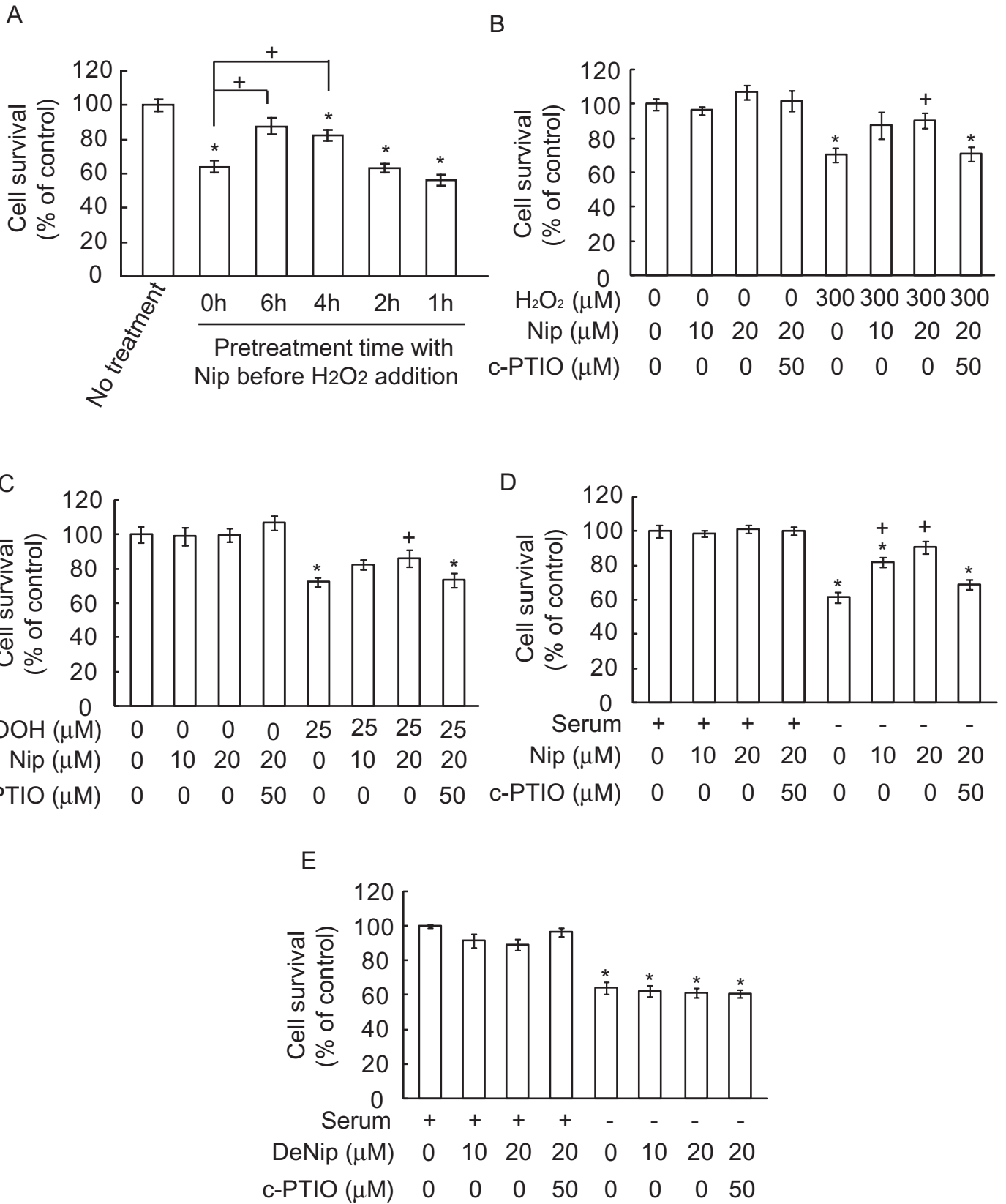


Fig. 3

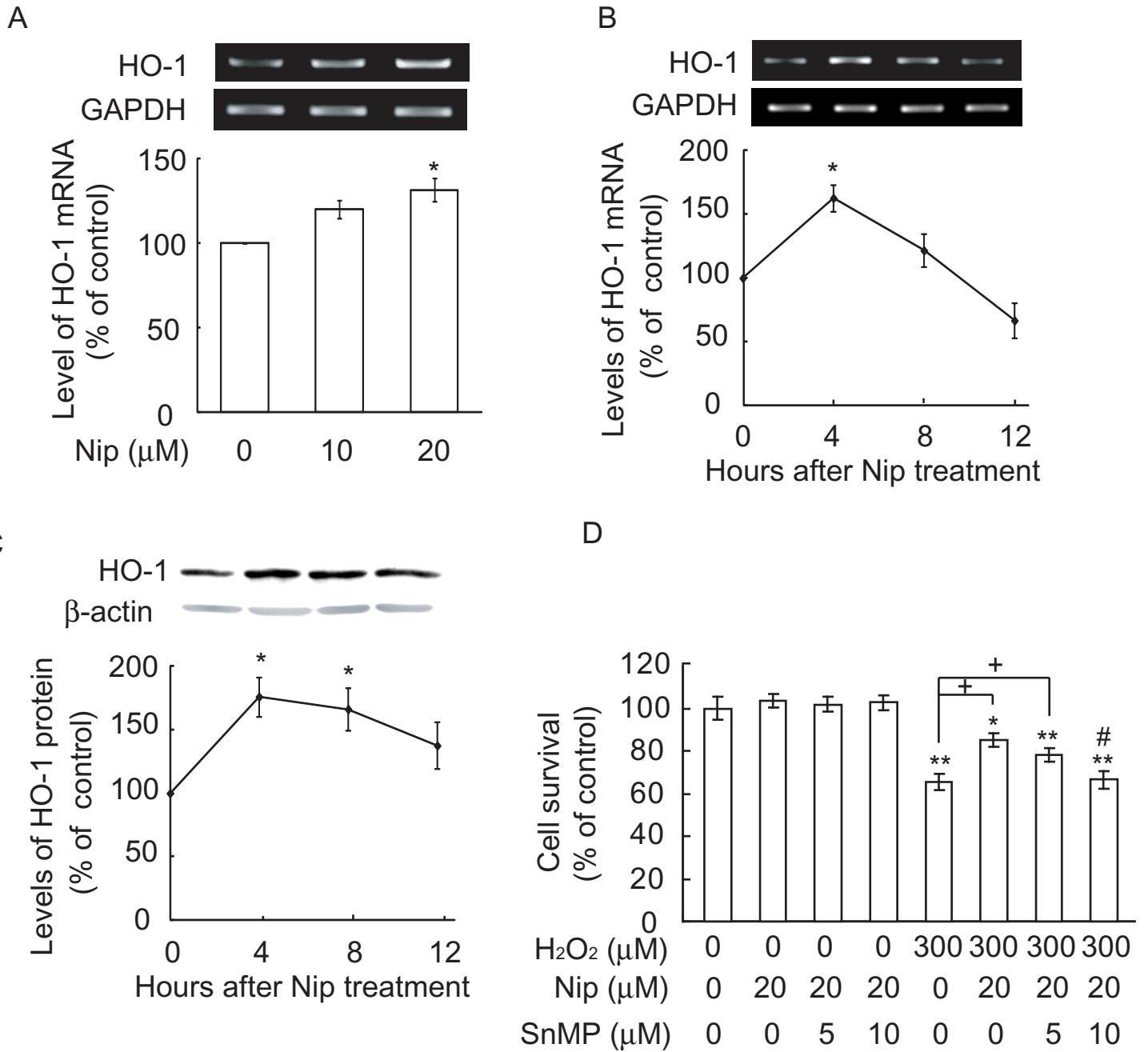
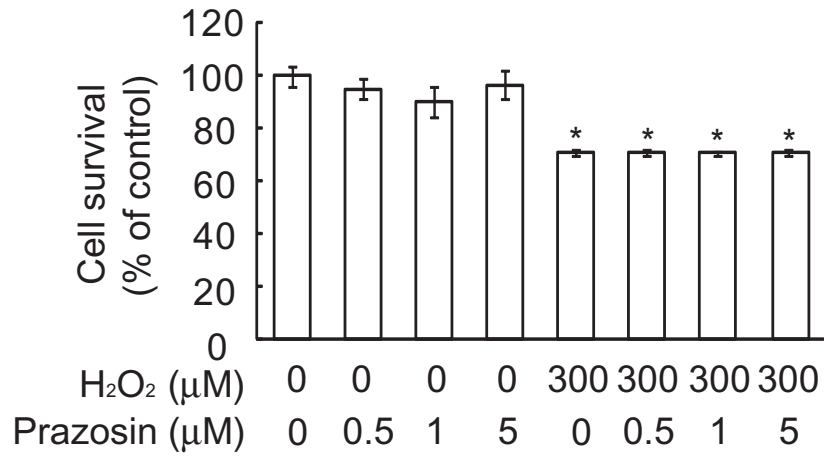
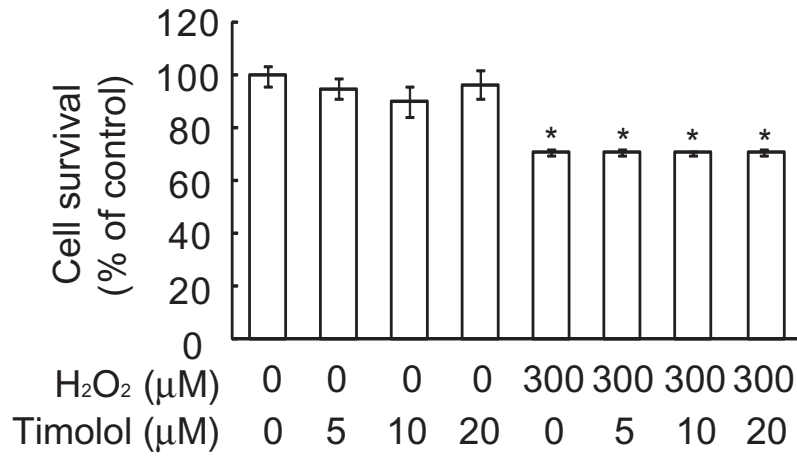


Fig. 4

A



B



C

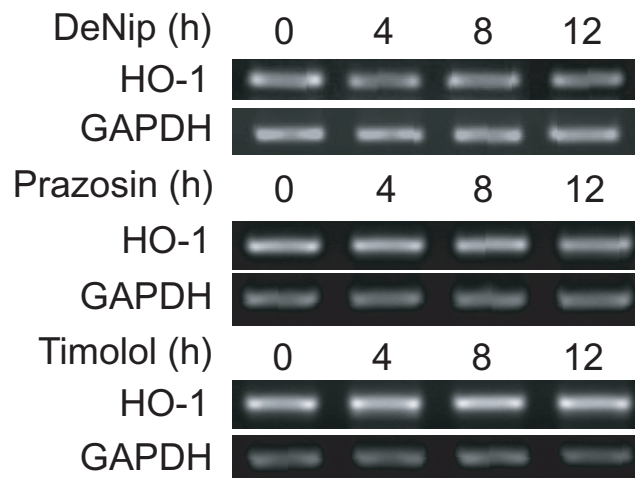
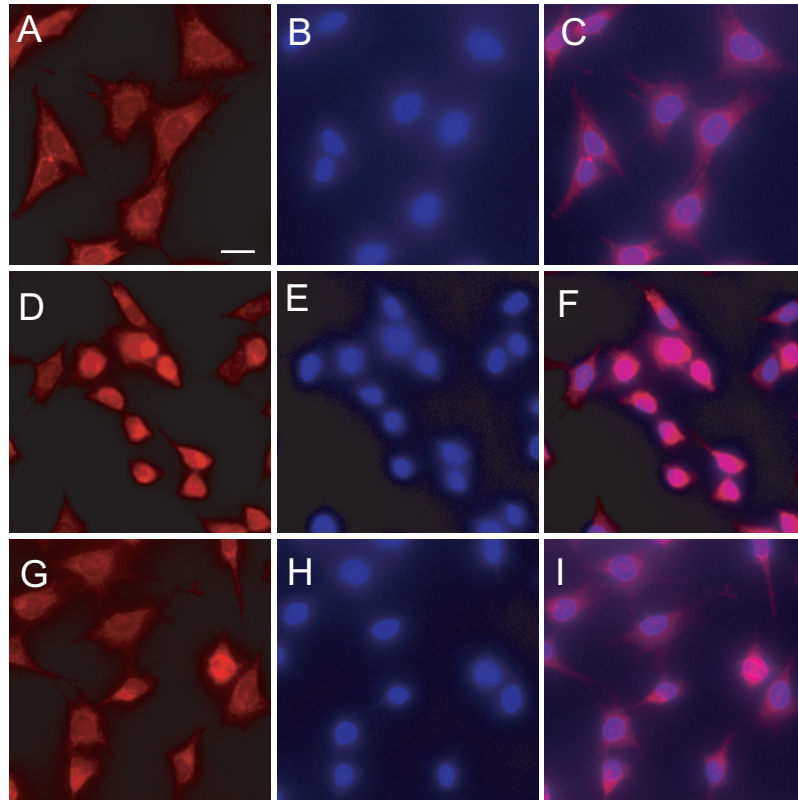
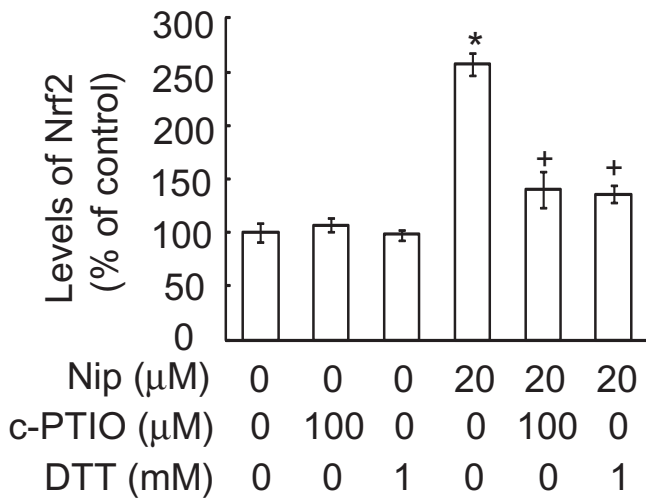


Fig. 5



J



K

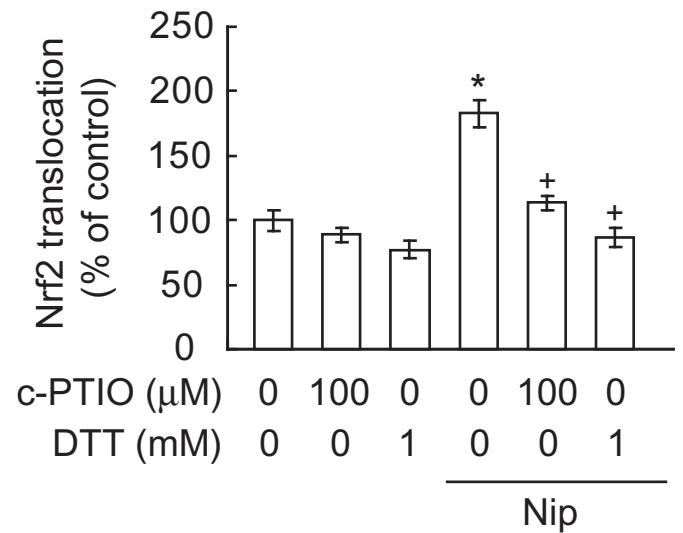


Fig. 6

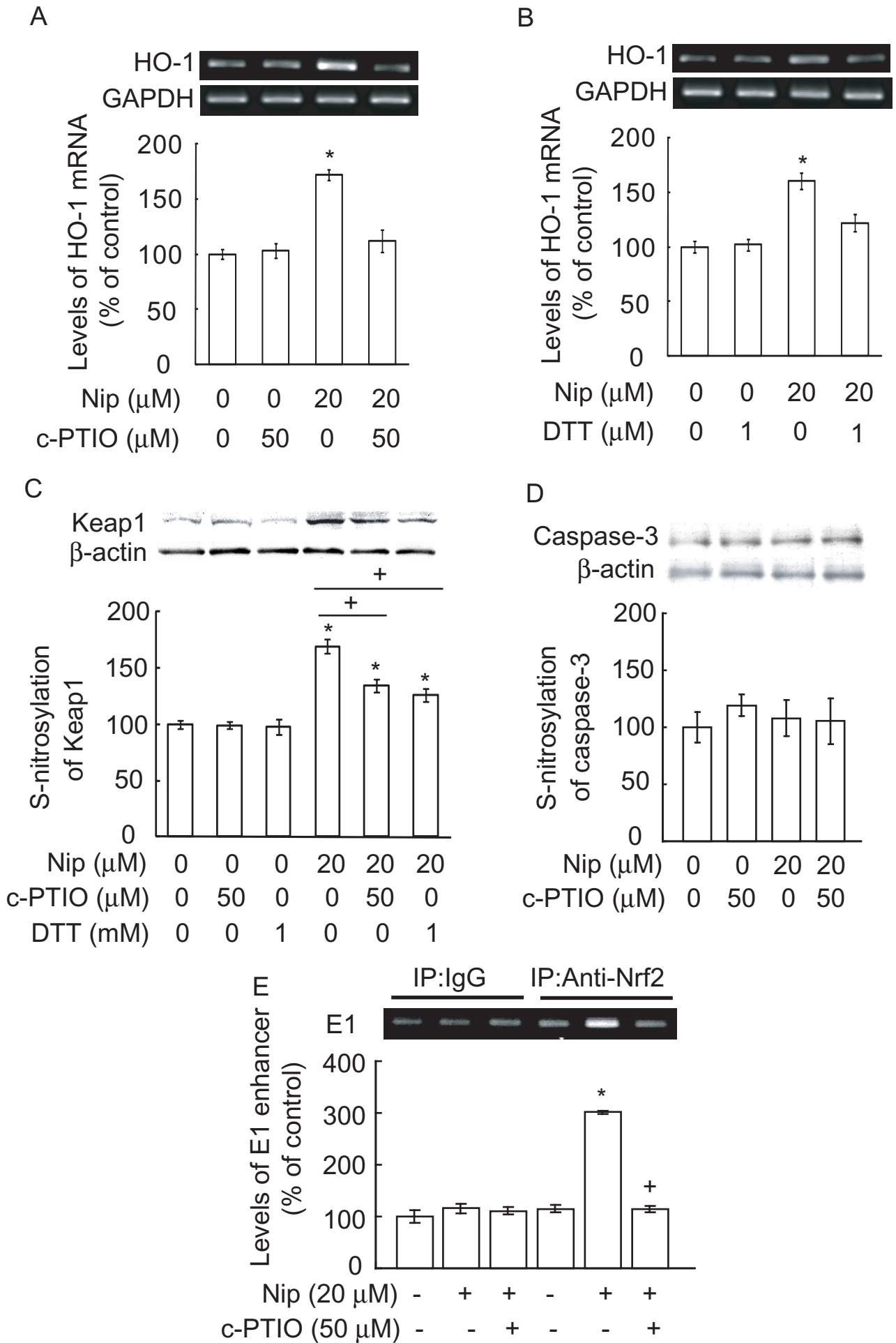
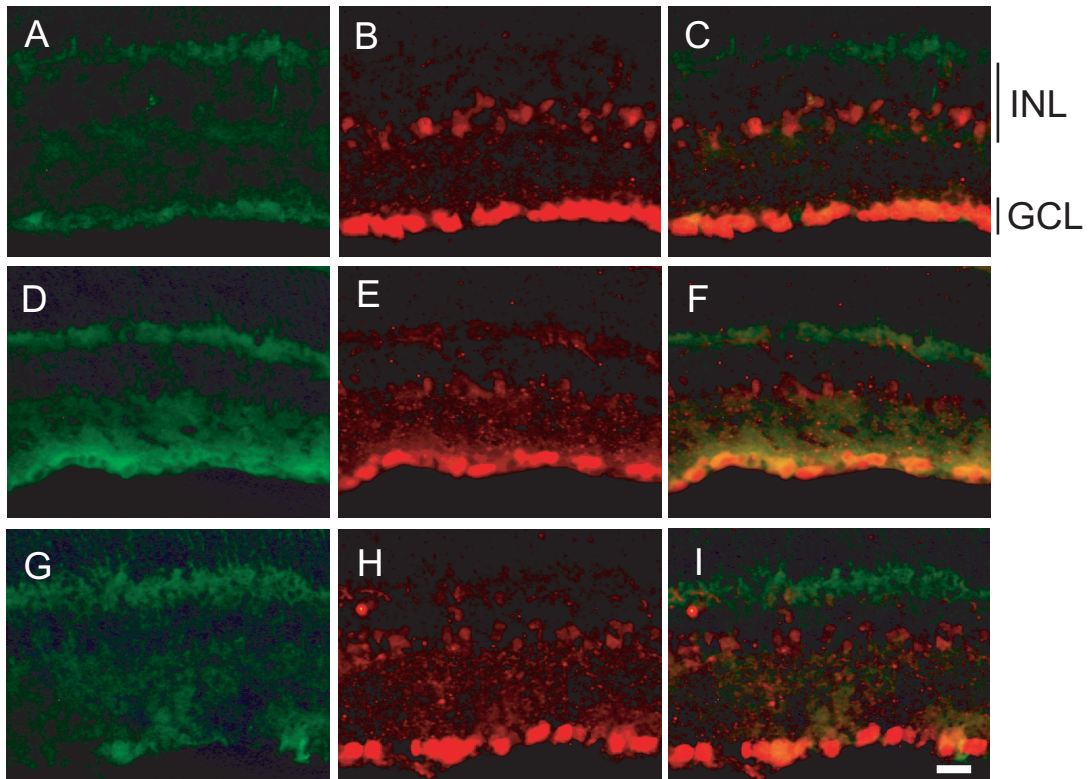
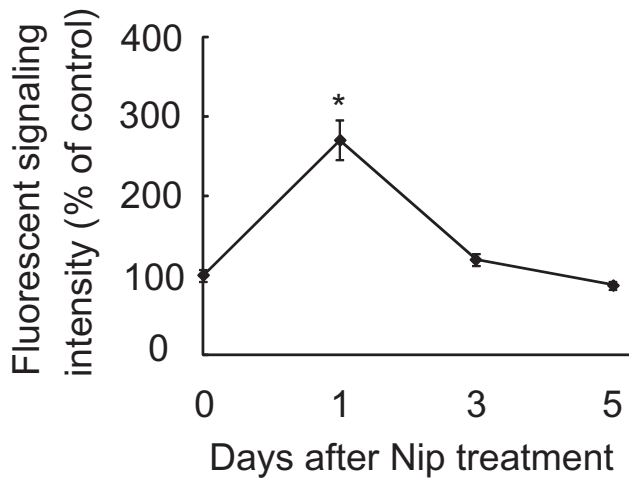


Fig.7



J



K

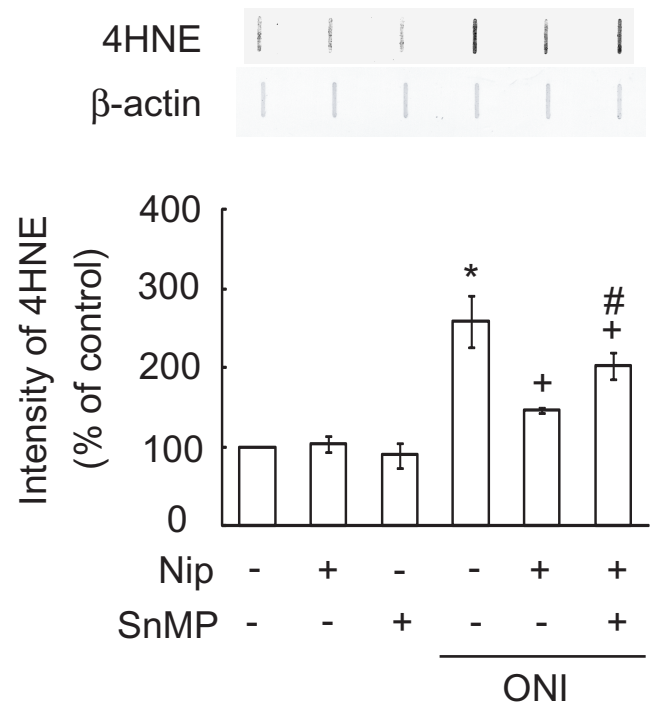


Fig. 8

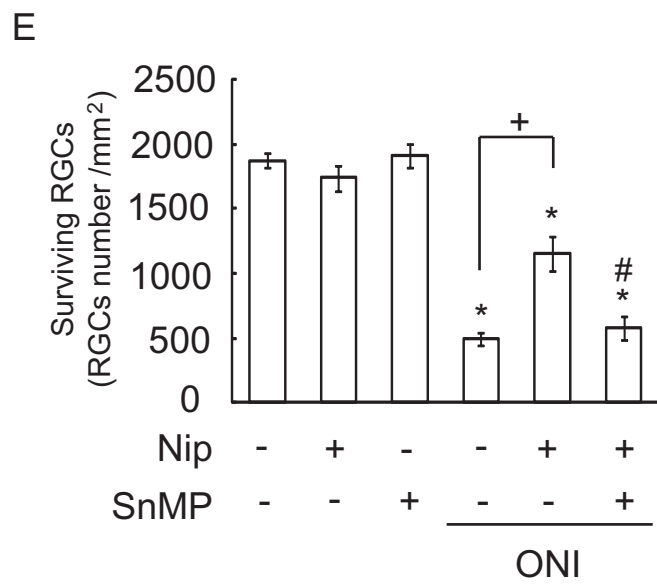
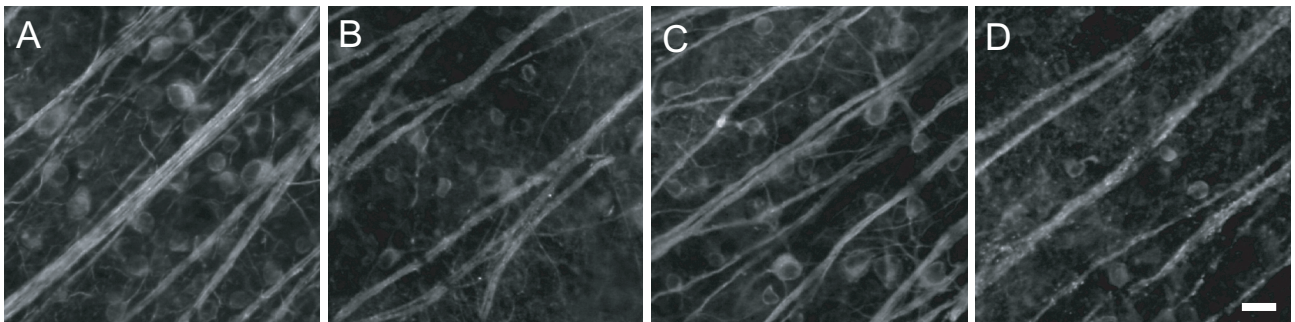


Fig. 9

